Desalination and Water Treatment
www.deswater.com
doi: 10.5004/dwt.2020.25169

182 (2020) 365–374
April

A sustainable and eco-friendly technique for dye adsorption from aqueous media using waste from *Jatropha curcas* (isotherm and kinetic model)

Musa Yahaya Pudza*, Zurina Z. Abidin*

Department of Chemical and Environmental Engineering, Universiti Putra Malaysia, 43400 Serdang, Selangor Darul Ehsan, Malaysia, emails: pudzamusa@gmail.com (M.Y. Pudza), zurina@upm.edu.my (Z.Z. Abidin)

Received 30 April 2019; Accepted 13 November 2019

ABSTRACT

The 21st century has witnessed a tremendous increase in textile wastewater effluent and consequently the pollution of water bodies that affects aquatic flora and fauna. This necessitates for a sustainable clean-up material to remove this contaminant. To realize this purpose, investigation of batch adsorption was conducted using Congo red (CR) as the adsorbate and *Jatropha curcas* seed (chaff) as the adsorbent material. Adsorption kinetics and isotherms analysis were conducted and results obtained confirmed the adsorption process as highly dependent on effects such as contact time, adsorbent dosage, initial dye concentration and the particle sizes of the adsorbate. The sorption equilibrium for CR dye unto *Jatropha curcas* seed (chaff) was achieved within 180 min and the adsorption efficiency was recorded at 82.05%. Furthermore, the result shows that the amount of CR adsorbed per unit mass of adsorbent increases from 11.47 to 82.05 mg/L as the initial concentration increase from 20–100 mg/L. Thus, the driving force for the CR adsorption gradient was due to the high adsorption capacity of *Jatropha curcas*. The process of the experimental sorption kinetics followed a pseudo-second-order kinetic model while the Freundlich and Langmuir isotherm model was both applicable for obtaining the equilibrium behavior of the adsorption. The chaff from *Jatropha curcas* seed possess carbonyl, acid amino and phenolic hydroxyl functional groups that act as chemical bonding agents for chemisorptions process at the surfaces of the adsorbent. This confirms the performance of *Jatropha curcas* (chaff) as an environmentally friendly and low-cost agromaterial for dye removal in aqueous solutions.

Keywords: Adsorption kinetics; Isotherm models; *Jatropha curcas*; Congo red

1. Introduction

From time immemorial, the need to preserve water resources has been indispensable to both the natural ecosystem and human developments, thus, wastewater generation cannot be avoided in most industries especially textile factories. The large industrial scale of wastewater purification involves the necessary use of adsorbent that is cheap to minimize the cost of large-scale industrial processes [1–3]. Much effort has been made to explore the possibility of using various low-cost adsorbent [4–6]. Literature has reported the use of low-cost biomaterial and biowaste to remedy water and wastewater including use of *Jatropha curcas* seed and press cake for turbidity removal [7], biosorption of Zn(II) [8], adsorption of methylene blue on waste potato peels unto chemically modified *Chaetophora elegans* algae [9,10], sequestration of reactive dyes using *Saccharomyces cerevisiae* [11], removal of copper (Cu(II)) from aqueous solution using algal biomass [12], water therapy utilizing chitosan mushroom [13] and also use of animal dung to treat industrial wastewater [14]. Furthermore, the negative environmental effects imposed on plants and animals [15,16]

* Corresponding authors.

when consuming chemicals for cleaning water and wastewater have escalated the growing interest in applying the previously mentioned low cost, environmentally sustainable and readily available material for effective water and wastewater treatment [1,17].

The elimination of color from wastewater is paramount before discharging it into any larger water body [18]. In view of the aforementioned, it becomes a daunting prerequisite to provide a suitable natural adsorbent that is environmentally sustainable to treat textile wastewater. It is necessary to find ways of safeguarding and maintaining a pristine water appearance.

Adsorption is one of the conventional and successful treatment processes, employed for dye removal from aqueous medium [19–21]. Adsorption is a physicochemical technique achieved by allowing the wastewater and the permeable material powder or granules to be in contact. By this technique, pollutants in the wastewater are effortlessly and promptly adsorbed and expelled onto the surface of the permeable material [22]. The process of adsorption involves the separation of a substance from one phase into another phase by adherence to the surface. Mostly there are two methods of adsorption which are physisorption and chemisorptions. Chemisorption takes place when the molecules in the liquid (or gas) phase become attached to the surface of the solid as a result of attractive forces at the solid surface (adsorbent) by overcoming the kinetic energy of the liquid contaminant (adsorbate) molecules while physisorption occurs when there is difference in energy or electrical attractive forces [23–26].

This work focuses on utilizing waste from agricultural material (*Jatropha curcas*) for efficient adsorption of color from wastewater. The waste generated from biodiesel productions and other applications of *Jatropha curcas* has become a source of concern, hence the waste (*Jatropha curcas* kernel) was utilized in this study for the treatment of textile effluent containing Congo red (CR) dye. Also, the characterization of the adsorbent by Brunauer–Emmett–Teller (BET), Fourier transform infrared (FTIR) and field emission scanning electron microscopy (FESEM) was observed with further isotherms, kinetics and regeneration studies.

2. Materials and methods

2.1. Method of preparing chaff from Jatropha curcas seed

The *Jatropha curcas* seeds were taken from Kaduna, north-central Nigeria. The seeds were manually harvested, dried under the sun and preserved in a moisture-proof container at 25°C–35°C and relative humidity of 40%–50% for two months. *Jatropha curcas* seed was then de-shelled manually and ground. 2 kg grounded shells were sieved at 1 mm particle size. Then it was kept in an airtight container for further usage.

2.2. Formulation of dye solution

CR sodium salt dye obtained from R&M marketing, Essex, U.K. has a molecular formula of $C_{32}H_{22}N_6Na_2O_6S_2$ with IUPAC name of disodium-4-amino-3-[4-[4-(1-amino-4-sulfonato-naphthalen-2-yl) diazenylphenyl]phenyl]diazenyl-naphthalene-1-sulfonate. A 1,000 ml stock solution was made by dissolving 1.0 g of CR in 1 L distilled water. To obtain various solutions, different concentrations were prepared by diluting the stock solution with a suitable volume of distilled water. All the reagents to be used were of analytical grade except otherwise stated.

2.3. Batch adsorption studies

The experiments were conducted under room temperature (25°C). A 250 mL stopper cork conical flasks were filled with 100 mL of adsorbate at different initial concentration (20–100 ppm), Contact time (3–180 min), pH (pH meter model Jenway 3305, England) ranging from 2 to 12, adsorbent dose (0.25–1.5 g), orbital sharker was set at a constant speed of 120 rpm (Model Heidolph, incubator 1000, Germany). Subsequently, the final concentration of dye was recorded by a double beam UV Spectrophotometer (Model GENESYS-10-UV) at a wavelength of 485 nm. The amount of adsorption at equilibrium, q_e (mg/g), was computed using Eq. (1) and the percentage removal of dye was calculated using the following Eq. (2) [21,27,28].

$$q_e = \frac{\left(C_0 - C_f\right)v}{M} \tag{1}$$

where q_e = adsorption capacity (mg/g); M = mass of the adsorbent used (g); V = volume of the dye solution (L).

$$\%\ \text{Removal} = \frac{C_0 - C_f}{C_0} \times 100 \tag{2}$$

where C_0 = initial dye concentration in sample (mg/L); C_f = equilibrium dye concentration in sample (mg/L).

2.4. Adsorption isotherm

Adsorption isotherm describes the equilibrium relationship between adsorbent and the adsorbate. These indicate the amount of adsorbate adsorbed by the adsorbent and the remaining adsorbate in aqueous solutions at a certain temperature [21]. The equilibrium isotherms were obtained graphically by plotting solid-phase concentration against liquid phase concentration [27,28].

2.4.1. Langmuir isotherm, adsorption equation and limitations

Langmuir isotherm is one of the most famous studies used for adsorption capacities [21] and it is based on four assumptions:

- Adsorption is monolayer.
- Specific homogenous when adsorption takes place within the adsorption site while the energy is constant and does not depend on the degree of occupation of adsorbents active center [29].
- All adsorption sites are equivalent to no interactions between adsorbate molecules on adjacent sites.
- Adsorption is reversible.

The following equation is the Langmuir isotherm equation [30].

$$q_e = \frac{q_{\max} K_L C_e}{1 + C_e K_L} \tag{3}$$

where q_e = adsorption capacity (mg/g); $q_{\max}$ = maximum monolayer adsorption capacity of the adsorbent (mg/g); C_e = equilibrium concentration of the adsorbate (mg/L); K_L = Langmuir adsorption constant related to free energy adsorption (L/mg).

Since the estimation of the adsorption isotherm parameters interference is by the method of linearization, therefore three (3) forms of isotherm equation are used to determine the constants K_L and $q_{\max}$. The three forms of Langmuir isotherm linearized equation are as follows [31,32].

Form 1:

$$\frac{C_e}{q_e} = \frac{1}{q_{\max} K_L} + \frac{C_e}{q_{\max}} \tag{4}$$

Form 2:

$$\frac{1}{q_e} = \frac{1}{q_{\max}} + \frac{1}{q_{\max} K_L C_e} \tag{5}$$

Form 3:

$$q_e = -\frac{q_e}{C_e K_L} + q_{\max} \tag{6}$$

Eqs. (4)–(6) are the derivation of the Langmuir isotherm model. It clarifies what happens at the equilibrium of the monolayer adsorption process. The number of molecules being adsorbed is equal to the number of molecules leaving the adsorbed state, that is the total amount absorbed $q_{\max}$ is directly proportional to the concentration in solution and available area for adsorption. Similarly, the rate of desorption is directly proportional to a number of molecules already adsorbed. At equilibrium, the rate of adsorption is equal to the rate of desorption [19].

The constants can be evaluated from intercept and the slope of linear plots of experimental data of (C_e/q_e) vs. C_e (Eq. (4)) or ($1/q_e$) vs. ($1/C_e$) (Eq. (5)) or q_e vs. (q_e/C_e) (Eq. (6)). The most popular form of analyzing adsorption equilibrium data is Langmuir Eq. (3) [33].

The essential characteristic of Langmuir isotherm may be expressed in terms of the dimensionless separation parameter R_L [34,35], which is an indication of isotherm shape that predicts whether an adsorption system is 'favorable' or 'unfavorable'. R_L is defined as:

$$R_L = \frac{1}{\left(1 + K_L C_0\right)} \tag{7}$$

where K_L is a Langmuir adsorption constant; C_0 is the initial concentration of dye.

The value of separation factor R_L indicates the adsorption process as given:

- Unfavourable ($R_L > 1$).
- Linear ($R_L = 1$).
- Favourable ($0 < R_L < 1$).
- Irreversible ($R_L = 0$).

2.4.2. Freundlich isotherm

The Freundlich isotherm is the earliest known relationship describing the sorption equation. This is a fairly satisfactory empirical isotherm which can be used for non-ideal sorption that involves heterogeneous surface energy system [36]. It is assumed that there are neither homogeneous site energies nor the limited level of sorption [29]. Freundlich isotherm equation is expressed by the following equation [37].

$$q_e = K_F C_e^{1/n} \tag{8}$$

where q_e = adsorption capacity (mg/g); K_F = Freundlich isotherm constant (mg/g); C_e = equilibrium concentration of adsorbate (mg/L); $1/n$ = adsorption capacity (L/mg).

To determine the constant K_F and n, equation (8) is linearized and used to produce a graph of $\ln q_e$ vs. $\ln C_e$ as follows:

$$\ln q_e = \ln K_F + \frac{1}{n} \ln C_e \tag{9}$$

K_F is the Freundlich proportionality constant obtained from the intercept and $1/n$ is from the slope. Here K_F represents the quantity of the absorbed CR requires to maintain CR concentration in the solution at unity (i.e. 1 mg/L). As K_F increases, the adsorption capacity for a given adsorbate also increases. The slope $1/n$ meanwhile ranges between 0–1 and when the value of $1/n$ gets closer to zero, the adsorption intensity or surface heterogeneity becomes more heterogeneous [19].

2.5. Regeneration studies

The spent *Jatropha curcas* adsorbent was regenerated by two regeneration cycles. First, the adsorbent was washed with deionized water three (3) times followed by washing in 0.1 M hydrochloric acid. Finally, the adsorbent was filtered, washed with deionized water and dried in an oven at 100°C for 5 h. The regeneration efficiency (RE%) was calculated from [19]:

$$\text{RE} = \frac{q_{\text{reg}}}{q_{\text{orig}}} 100\% \tag{10}$$

where q_{reg} and q_{orig} are the adsorption capacities per unit of mass of the regenerated and the original adsorbent respectively.

2.6. Characterization of adsorbent (Jatropha curcas)

The surface area and pores size distribution were obtained using the BET equipment (SA-9600 series). The FTIR analysis was performed on the samples to determine the surface functional groups in range 4,000–500 cm^{-1}. A PerkinElmer Spectrum (100 FTIR spectrometer) with PIKE MIRACLE

(Llantrisant, CF72 8YW, United Kingdom (UK)) attenuated total reflection attachment was used to record the spectra. The FESEM (Hitachi Co., Japan, Model No. S3400N) was used to obtain images of *Jatropha curcas* at high resolutions.

3. Results and discussion

3.1. Characterization of powdered chaff

3.1.1. Fourier transform infrared (FTIR)

The mechanism for adsorption by powdered chaff of *Jatropha curcas* depends on the chemical reactivity of functional groups on the surface. This reactivity creates an imbalance between forces at the surface compared to inside the body thus leading to molecular adsorption by the Van der Waals force. Knowledge of surface functional groups would give information to the adsorption capability of the produced powder chaff. FTIR spectra were collected for qualitative characterization of surface functional groups of the chaff of *Jatropha curcas* seed. Fig. 1, shows the functional groups of the powder chaff. The peaks at 3,312–3,781 cm^{-1} in spectra of *Jatropha curcas* chaff were assigned to the alcohol group (–OH) stretching which has strong, sharp and broad intensity. The band at 2,855–3,008 cm^{-1} can be attributed to the acid group (O–H) stretch which has a strong and broad intensity. The amide and ester group which contain a carbonyl (C=O) is assigned at the peak 1,660 and 1,745 cm^{-1} respectively which have a strong intensity. The adsorption peak at 1,000–1,300 cm^{-1} refers to the ester group (C–O) stretching which has two or more band intensity [27,38].

From the FTIR analysis in Fig. 1 (before and after), it is concluded that the powder chaff from *Jatropha curcas* seed has a broad and strong (O–H) stretching which indicates the presence of strong hydrogen bonds associated with alcohols and carbonyl. Thus, the carbonyl, acid amino and phenolic hydroxyl act as a chemical bonding agent for chemisorptions which indicated that adsorption of CR on powdered chaff involved electrostatic attraction especially interaction between the dye and the carboxylate and phenolic hydroxyl groups on the powdered chaff of *Jatropha curcas* [37,39].

3.1.2. FESEM analysis

The FESEM image of the chaff of *Jatropha curcas* seed shows an irregular surface with a large porous surface area (see Fig. 2a). The adsorption of CR leads to multiple attachments on the rough surface and occupation of pores (Fig. 2b). Pores in a solid medium like adsorbents may have properties such as shape, location, connectivity, and surface chemistry [40]. Fig. 2b meanwhile displays the pores for adsorption of CR which have been occupied according to a zigzag pattern as reported by other researchers [11].

3.1.3. BET analysis

The BET analysis of the adsorbent (*Jatropha curcas*) offers an insightful analysis of the specific surface area, pore size and pore volume of the *Jatropha curcas* that are available for explaining the adsorption of CR. Table 1 provides the BET data that is believed to be responsible for the efficiency of *Jatropha curcas* as an adsorbent.

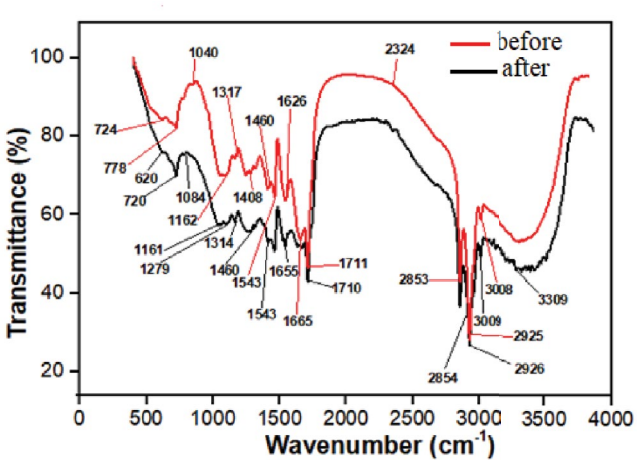

Fig. 1. Fourier transform infrared (FTIR) analysis of *Jatropha curcas* before and after adsorption of CR.

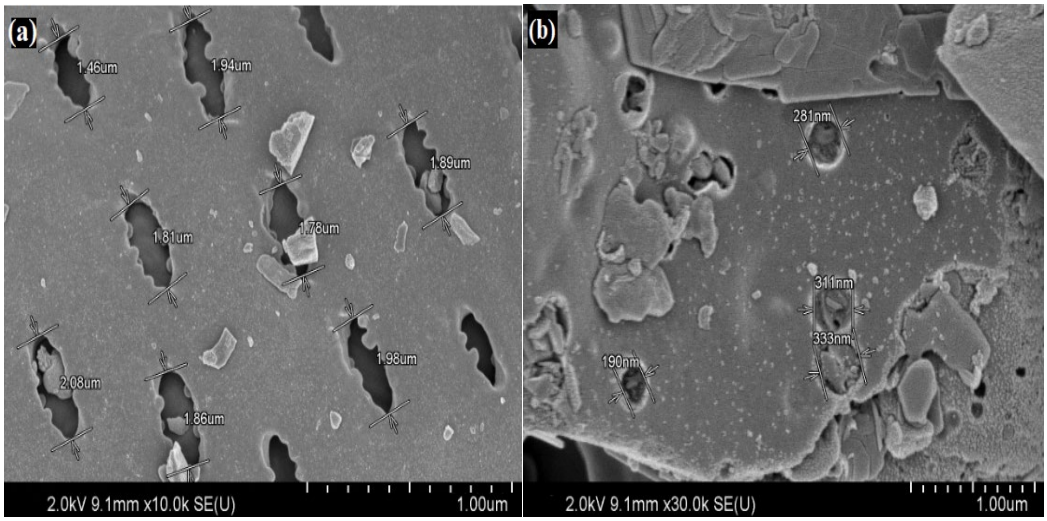

Fig. 2. FESEM images for chaff *Jatropha curcas* seed (a) before and (b) after adsorption.

Table 1
BET analysis of *Jatropha curcas*

Adsorbent	SSA (m^2/g)	Pore volume (m^3/g)	Pore size (Å)
Jatropha curcas before adsorption	687.4455	0.98297	28.6726
Jatropha curcas after adsorption	47.3968	0.1339	68.7848

The adsorbent before adsorption exhibits a high surface area of 687.4455 m^2/g as a result of good carbonization, activation and subsequent modification. These results implied that there are abundant surface areas for the adsorption to occur. The adsorption capacity of *Jatropha curcas* depends on the availability of the pore volume and the range of time taken for the adsorption process. For adsorption time the pores became saturated due to the deposition of adsorbate on the surface. The specific surface area of the adsorbent after adsorption depicts that there is general pore reduction (47.3968 m^2/g) when compared to the fresh adsorbent. Similar findings can be found in other literature [36].

3.2. Batch adsorption studies

The adsorption efficiency was investigated with respect to the effect of CR initial concentration, pH, dosages and temperature.

Fig. 3a depicts the effect of CR concentration and phases contact time at different initial concentrations of CR stock solution. Initial concentrations were varied between 20 to 100 mg/L while the dosage was kept constant. The rate of adsorption was higher in the beginning due to the availability of larger surface area on the adsorbent [41–43]. These strong attractive forces that occurred between the adsorbate and adsorbent surfaces help the intra-particle matrix to attain rapid equilibrium [41]. As contact time increased, the adsorption rate became slower since the adsorbent become saturated thus restricting solute diffusion through the adsorbent. For most of the initial concentration, the equilibrium was attained after 60 min out of the total experimental period of 3 h. The result shows that the amount of CR adsorbed per unit mass of adsorbent increases from 11.47 to 82.05 mg/L as the initial concentration increase from 20–100 mg/L. When the concentration of CR increased, the driving force due to the large concentration gradient was stronger because of the higher adsorption capacity [27]. As earlier stated the time to reach relative saturation was at 60 min which are in agreement with previous research [42].

The effect of pH on CR was studied at various initial pH under equilibrium contact time (3 h), the concentration of CR solution (50 mg/L) and dosage of adsorbent (1 g). The results are as shown in Fig. 3b. The percentage dye removed by *Jatropha curcas* was lower at high pH (4.09% at pH 11) and higher at pH 3 (84.02%). This is because, at pH 3, the *Jatropha curcas* exhibits a zeta potential value of +9.2 mV [7], which suggests the existence of a positive charge on the surface of

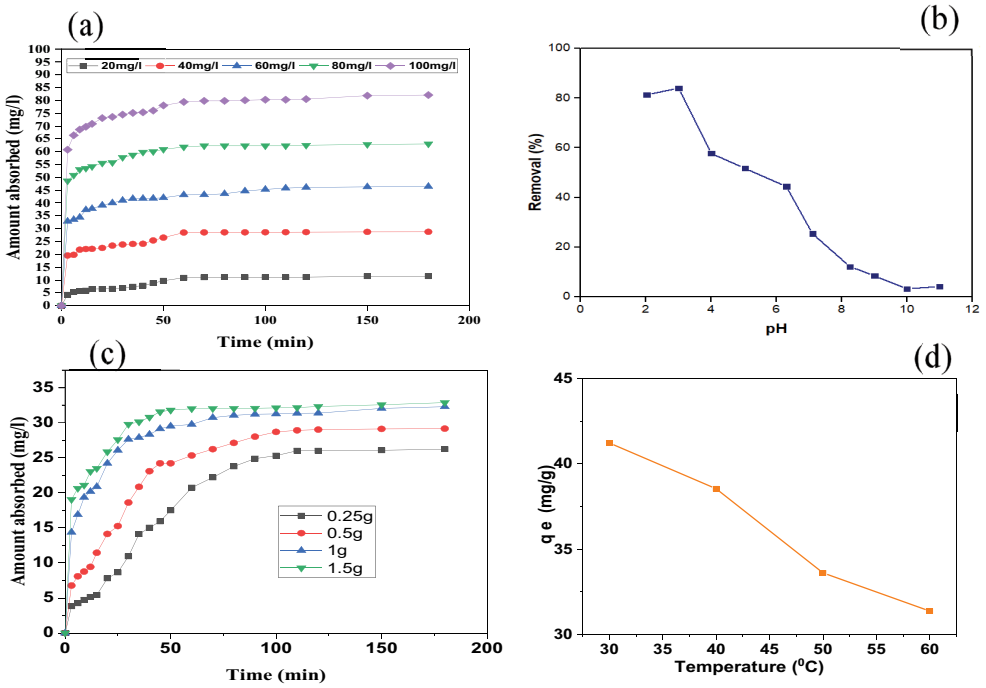

Fig. 3. Batch adsorption study (a–d). (a) Effect of CR concentration against phases contact time, (b) percentage removal of CR at different pH, (c) effect of adsorbent dose against phases contact time, and (d) effect of temperature on *Jatropha curcas* adsorption efficiency.

Jatropha curcas adsorbent which is known to compose mainly of protein. Thus, it easily adsorbed the negatively charge CR anion CR [44]. Protein is made up of a chain of amino acids that has an isoelectric point (pI) values from 3 to around 11. Below the isoelectric point, positive charge dominates while above the isoelectric point negative charge persists. Hence, at acidic pH, most amino acids that build up the protein possess positive charges. As an amphoteric molecule, the charge on the protein is greatly influenced by the pH values. It is believed that the main mechanism molecules interaction is through adsorption and neutralization of charges. *Jatropha curcas* is an adsorbent agent that works effectively under highly acidic conditions, though, it is relevant for treating industrial wastewater with a variable pH [8].

The amount of *Jatropha curcas* used to remove CR was varied from 0.25 to 1.5 g for investigation of the relationship between adsorbent dosages on the amount of adsorbate removed. The influence of sorbent dose on adsorption enables the determination of the highest equilibrium adsorption capacity. In this study, when the adsorbent dose was increased from 0.25 to 1.5 g, there was a significant decrease in the equilibrium of CR uptake. This is shown in Fig. 3c where an increase in adsorbent dose increases the available adsorption sites. On top of that, overlapping of adsorption sites also happened and this can inhibit adsorption of more CR dye molecules over time. Previous studies for the effect of adsorbent dose on CR dye adsorption by eucalyptus wood and jujube seeds have shown similar findings [28].

Temperature changes the number of dye molecules in solution, viscosity and the surface characteristics of the adsorbent. This particular influence of temperature on the adsorption of CR onto *Jatropha curcas* was observed, within the temperature range of 303–333 K. As shown in Fig. 3d, the adsorption of CR dye unto the adsorbents understudy is exothermic. Therefore, an increase in temperature weakens intermolecular hydrogen bonding and Van der Waal forces between dye molecules and functional groups on the adsorbent surface [32,45]. Similar observations have been reported on spent brewery grains and activated lignin-chitosan for adsorption [46,47].

3.3. Regeneration studies

It is essential to be conscious of the waste that is generated as a byproduct of any sustainable action [48]. For this reason, the *Jatropha curcas* was reused to ensure the economical and feasibility of its application in the adsorption treatment of water polluted by CR. This regeneration investigation was performed in five adsorption/desorption cycles. The chemical desorption of *Jatropha curcas* with 0.1 HCl concentrations showed high efficiency which is in agreement with recent literature [19] as shown in Fig. 4. Overall, the CR removal was slightly decreased from 95% to 81% (as shown in Fig. 4), after five cycles for 0.1 mol/L concentration of HCl, which is less than 10% efficiency reduction indicating good performance and its suitable capabilities for large scale application.

3.4. Adsorption equilibrium

The adsorption isotherm gives clarity on the nature and mechanism of the adsorption process. The experimental

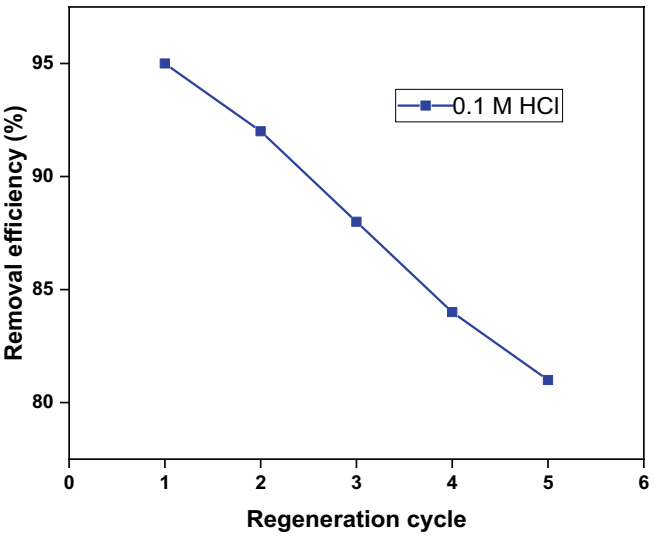

Fig. 4. Reusability of *Jatropha curcas* for CR adsorption.

conditions for adsorption isotherms were; pH = 3, dosage = 1 g, temperature = 25°C, time = 180 min. The Langmuir model (Eq. (3)) describes how the mechanism of adsorption at homogeneous sites happens by the effect of the monolayer adsorption process without any interaction between the adsorbed molecules [49]. Based on Eq. (3), a plot of q_e vs. C_e is plotted and can be seen in Fig. 5. The general classification system of adsorption divides all isotherms into four main classes according to the initial slope, and sub-groups that describes each class, based on the shapes of the upper parts of the curves. The four main classes are named the S, L (i.e. Langmuir type as in Fig. 5), H (high affinity), and C (constant partition) isotherms, and the variations in each class are divided into sub-groups. The L curves (Fig. 5) are the best known and indeed the L curve occurs in probably

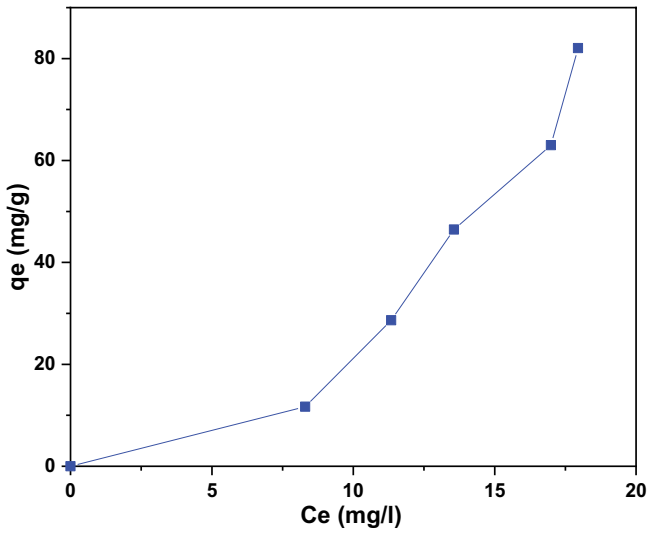

Fig. 5. Adsorption equilibrium isotherm of CR into *Jatropha curcas*. (pH = 3, dosage = 1 g, temperature = 250°C, time = 180 min, initial concentration range = 20, 40, 60, 80, and 100 mg/L).

the majority of cases of adsorption from dilute solution while few cases of the other types appear to have been previously recorded [50,51].

3.4.1. Langmuir isotherm

The Langmuir isotherm model is a known model for describing the adsorption process of a homogeneous nature. This process was obtained at experimental conditions of pH = 3, dosage = 1 g, temperature = 25°C, time = 180 min. The Langmuir isotherm parameters q_{max} and K_L were determined from slope and intercept of the plots of the Langmuir model as mentioned earlier as Form 1, 2 and 3 (Table 2) [25,34,43,47–49]. The linearized forms of Langmuir isotherms are expressed in Fig. 6.

Figs. 6a–c shows the linearized form of the Langmuir isotherms for CR adsorption unto *Jatropha curcas* at experimental conditions of pH = 3, dosage = 1 g, temperature = 250°C, and time = 180 min. The values of the Langmuir constant K_L and the monolayer capacity q_{max} can be evaluated from three forms of Langmuir adsorption models. This can be done either way from the intercept and the slope of the linear plot

Table 2
Parameters and separation factors (R_L) for the three Langmuir forms

Adsorbent	Langmuir isotherm form	q_{max} (mg/g)	K_L	R^2	R_L
Jatropha curcas	1	–22.2974	–0.04538	0.9274	0.0209
	2	–18.5087	–0.04431	0.9965	0.0209
	3	–24.2337	–0.04431	0.9673	0.0209

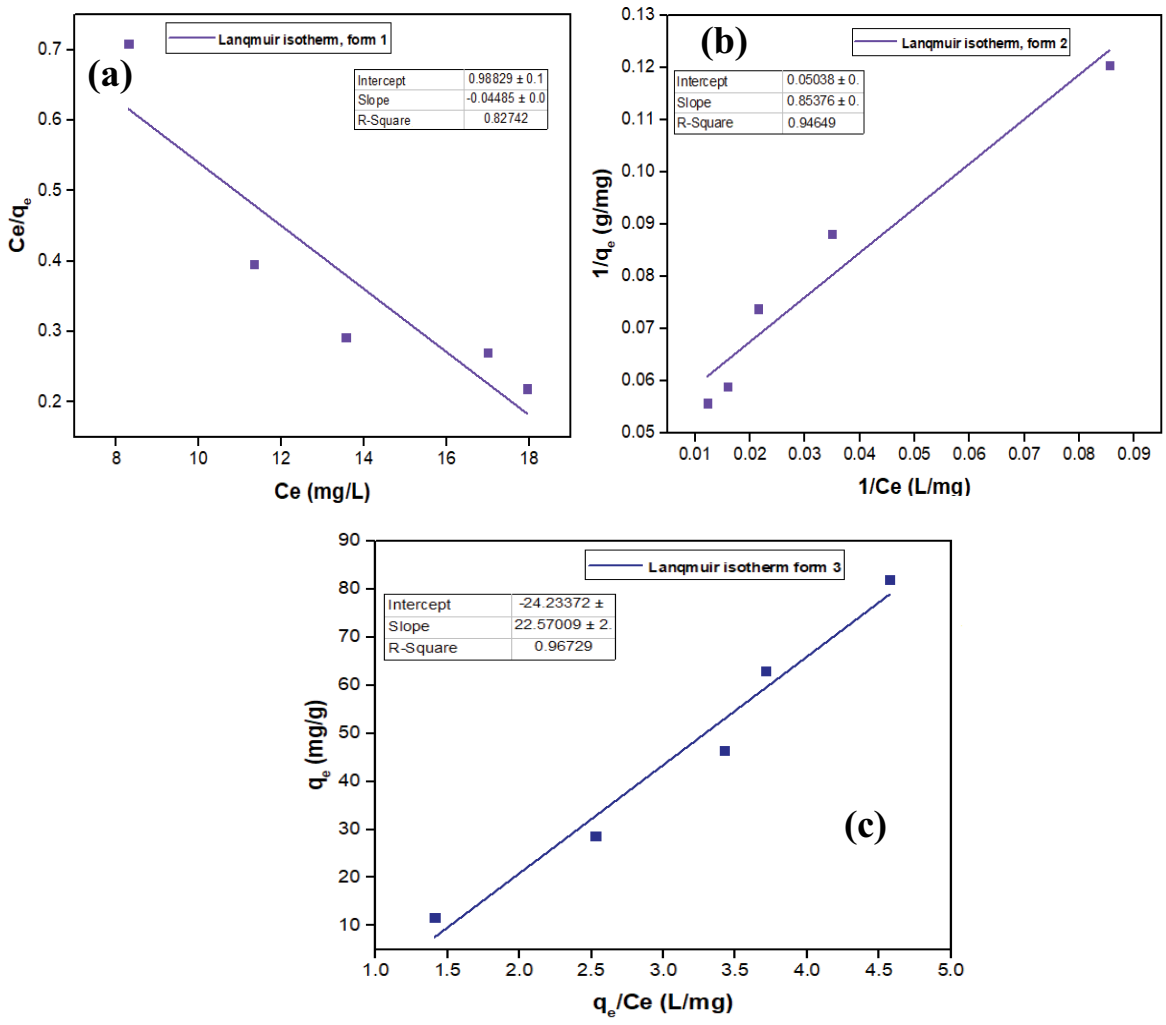

Fig. 6. Linearized forms of Langmuir isotherm (a) form 1, (b) form 2, and (c) form 3.

of the experimental data (C_e/q_e) vs. C_e (Eq. (4)) or ($1/q_e$) vs. ($1/C_e$) (Eq. (5)) or q_e vs. (q_e/C_e) (Eq. (6)).

By comparing the three Langmuir forms in Table 2 and Figs. 6a–c, it was validated that Langmuir Form 2 has higher correlation coefficients R^2 than other Langmuir forms which are an indication that the Langmuir form 2 fits best to the adsorption process when compared to Langmuir equation form 1 and 3. All the *R*-values for the adsorption of CR on *Jatropha curcas* are found to be closer to unity (1), which shows that the adsorption process is favorable, this is due to the effect of the pore diffusion sorption phenomenon [27].

3.4.2. Freundlich isotherm

The Freundlich adsorption isotherm is the relationship between the concentrations of CR on the surface of *Jatropha curcas* to the concentration of CR in the bulk liquid with which it is immersed. The plot of ln q_e against lnC_e is shown in Fig. 7 which provides a straight-line graph and the values of $1/n$ and K_F were obtained from the slope and the interception. The slope ($1/n$) from 0 to 1 is a measure of adsorption intensity or surface uniformity and indicates more uniformity as its value gets closer to zero [33]. If the value of exponent n is greater than 1 ($n > 1$) then the adsorption is said to represent favorable adsorption conditions [2,52]. The values of n and K_F are listed in Table 3.

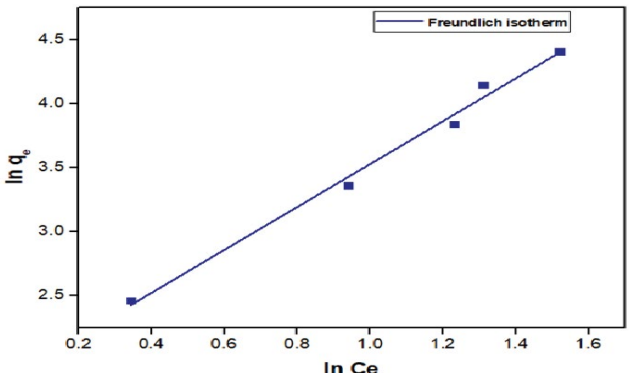

Fig. 7. Linearized form of Freundlich isotherm (pH = 3, dosage = 1 g, temperature = 250°C, time = 180 min, initial concentration range = 20, 40, 60, 80 and 100 mg/L).

The Freundlich isotherm parameters of K_F and n were found as 0.082 and 1.69, respectively with R^2 = 0.9913. The value of $1/n$ is 0.592 which indicates heterogeneity of *Jatropha curcas* surface. However, R^2 of Freundlich isotherm (09913) is only slightly lower than Langmuir Form 2 (0.9965). Hence, it is deduced that both isotherms can describe the adsorption process satisfactorily and it is believed that both physisorption and chemisorption occur during the adsorption process.

3.5. Adsorption kinetics

The adsorption experiment was carried out at a concentration of 20–100 ppm, at pH 3, adsorbent dose of 1 g and contact time varied between 3 to 180 min.

In this model, the Lagergren equation was used in the determination of the rate constant for adsorption of CR. A graph of t/q_t against t was plotted to show the trend of this model. Fig. 8 (first and second-order kinetic model) shows a linear form of CR concentration on *Jatropha curcas*. The adsorption phenomenon of CR and *Jatropha curcas* fitted the pseudo-second-order kinetic model with an R^2 coefficient of 0.9855 and 0.9996 at 20 and 100 mg/L respectively. The calculated values of adsorption capacity ($q_{cal.}$) is higher than the first model. The value ranges from 12.36 to 82.65 mg/g for 20 and 100 mg/L. Based on the observed calculated and experimental values, it can be concluded that the adsorption of CR follows the pseudo-second-order kinetic model [15].

Pseudo-second-order rate constant (k_2), and q_e, and $q_{cal.}$ were obtained from the slope and intercept of the graph in Fig. 8. From Table 4, it can be seen that the $q_{e,cal.}$ values calculated from the pseudo-second-order kinetic model show compatibility trend as compared to the experimental uptake ($q_{exp.}$).

Furthermore, R^2 values for each concentration from (20–100 mg/L) in pseudo-second-order kinetic model are higher (>0.98) than those obtained in pseudo-first-order kinetic model. This phenomenon reveals that the adsorption process does rightly fits into the pseudo-second-order kinetic model [19,29,53,54].

Table 3
Freundlich isotherm parameters for CR adsorption onto *Jatropha curcas*

Isotherm	n	$1/n$	K_F ((mg/g) (L/mg)$^{1/n}$)	R^2
Freundlich	1.69	0.592	0.082	0.9913

Table 4
Kinetic study of CR absorption by *Jatropha curcas* pseudo-first-order model and pseudo-second-order model

C_0	R^2	$q_{e,cal.}$ (mg/g)	$q_{e,exp.}$ (mg/g)	R^2	$q_{e,cal.}$ (mg/g)	$q_{e,exp.}$ (mg/g)
20	0.9056	8.25	11.47	0.9855	12.36	11.47
40	0.9063	14.81	28.76	0.9979	29.58	28.76
60	0.9074	16.34	46.44	0.999	46.94	46.44
80	0.8792	15.215	63.01	0.9998	63.69	63.01
100	0.8363	19.05	82.05	0.9996	82.64	82.05

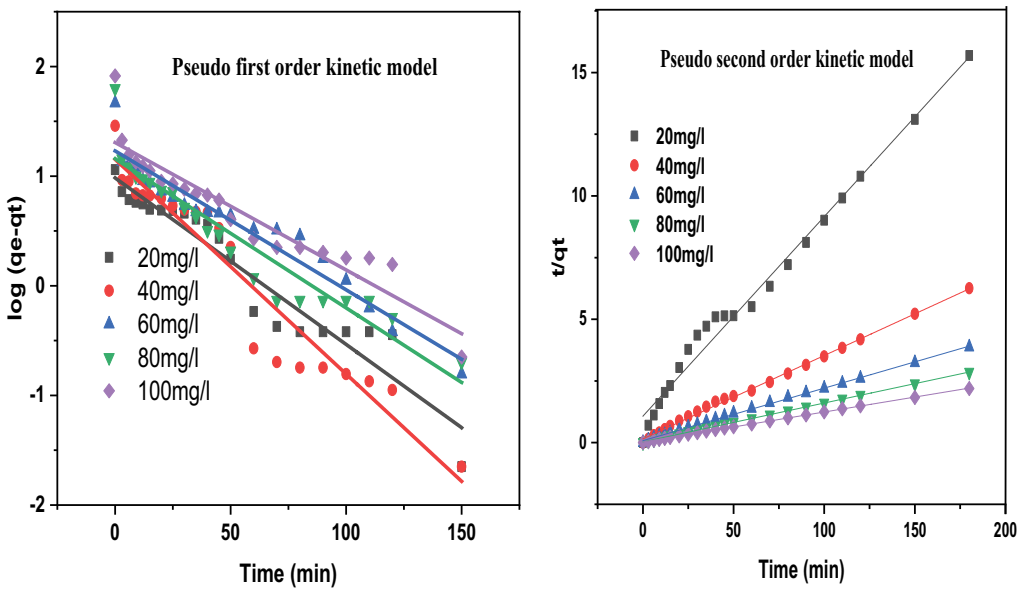

Fig. 8. Kinetic models for pseudo-first-order and pseudo-second-order adsorption of CR on *Jatropha curcas*.

4. Conclusion

The experimental finding in this work suggests that *Jatropha curcas* is a potential cost-effective adsorbent and a remedy for treating wastewater contaminates with dyes. Result have confirmed that the amount of CR adsorbed per unit mass of adsorbent increased as a function of time and also initial CR concentration. Higher adsorption capacity of the adsorbent is favourable at acidic pH. The process of the experimental sorption follows a pseudo-second-order kinetic model while Langmuir (R^2 = 0.9965) and Freundlich (R^2 = 0.9913) isotherm models were both applicable for obtaining the equilibrium of the parameters, with the adsorption process slightly favourable towards the Langmuir adsorption process. This is an indication of the occurrence of physisorptions, chemisorptions and electrostatic interactions. Existence of carbonyl, acid amino and phenolic hydroxyl groups on the powdered chaff acts as chemical bonding agents for favorable chemisorptions process. This is further supported by availability of irregular highly porous surface area on the adsorbent. This confirms *Jatropha curcas* performance as an environmental friendly and low-cost agro waste for dye removal in aqueous solutions.

Acknowledgment

The authors would like to thank the Malaysian Ministry of Higher Education for sponsoring the work under Fundamental Research Grant Scheme (03-02-13-129FR) and Master of Environmental Engineering for sponsoring the work.

References

[1] M.L. Mathew, A. Gopalakrishnan, C.T. Aravindakumar, U.K. Aravind, Low–cost multilayered green fiber for the treatment of textile industry wastewater, J. Hazard. Mater., 365 (2019) 297–305.
[2] S.F. Azha, L. Sellaoui, M.S. Shamsudin, S. Ismail, A. Bonilla-Petriciolet, A.B. Lamine, A. Erto, Synthesis and characterization of a novel amphoteric adsorbent coating for anionic and cationic dyes adsorption: experimental investigation and statistical physics modelling, Chem. Eng. J., 351 (2018) 221–229.
[3] W. Rudzinski, W. Plazinski, Theoretical description of the kinetics of solute adsorption at heterogeneous solid/solution interfaces: on the possibility of distinguishing between the diffusional and the surface reaction kinetics models, Appl. Surf. Sci., 253 (2007) 5827–5840.
[4] T.W. Leal, L.A. Lourenço, A.S. Scheibe, S.M.G.U. de Souza, A.A.U. de Souza, Textile wastewater treatment using low-cost adsorbent aiming the water reuse in dyeing process, J. Environ. Chem Eng., 6 (2018) 2705–2712.
[5] P. Nautiyal, K.A. Subramanian, M.G. Dastidar, Adsorptive removal of dye using biochar derived from residual algae after in-situ transesterification: alternate use of waste of biodiesel industry, J. Environ. Manage., 182 (2016) 187–197.
[6] K. Singh, B. Chandra, M. Gautam, Developement of inexpensive adsorbent from agro-waste for phenol adsorption, J. Sci. Ind. Res., 86 (2016) 444–451.
[7] Z.Z. Abidin, N. Madehi, R. Yunus, Coagulative behavior of *Jatropha curcas* and its performance in wastewater treatment, Environ. Prog. Sustainable Energy, 36 (2017) 126–135.
[8] Z.Z. Abidin, M. Salleh, M.Y. Harun, A.N. Bakar, Biosorption of Zn(II) from aqueous solution by *Jatropha curcas* press cake, J. Sci. Ind. Res., 78 (2014) 191–194.
[9] A.O. Yalcyn, G.P.S. Selda, A. Nevin, The adsorption of Methylene blue from aqueous solution by using waste potato peels; equilibrium and kinetic studies, J. Sci. Ind. Res., 51 (2012) 817–821.
[10] F. Mikati, M.E. Jamal, Biosorption of methylene blue on chemically modified *Chaetophora elegans* algae by carboxylic acids, J. Sci. Ind. Res., 96 (2013) 428–434.
[11] E.S. Bireller, P. Ayater, S. Gedikli, A. Cabuk, Removal of some reactive dyes by untreated and pretreated *Saccharomyces cerevisiae*, an alcohol fermentation wate, J. Sci. Ind. Res., 94 (2012) 632–639.
[12] N.R. Bishnoi, A. Pant, Biosorption of copper from aqueous solution using algal biomas, J. Sci. Ind. Res., 53 (2004) 813–816.
[13] V. Sheoran, R. Chaudharr, N.K. Tholia, Treatment of industrial waste by organic wastes, J. Sci. Ind. Res., 21 (2013) 255–260.
[14] O. Adnan, Z.Z. Abidin, A. Idris, S. Kamarudin, M.S. Al-Qubaisi, A novel biocoagulant agent from mushroom chitosan as water and wastewater therapy, Environ. Sci. Pollut. Res., 24 (2017) 12–17.

[15] W. Astuti, T. Sulistyaningsih, E. Kusumastuti, G.Y.R.S. Thomas, R.Y. Kusnadi, Thermal conversion of pineapple crown leaf waste to magnetized activated carbon for dye removal, Bioresour. Technol., 287 (2019) 121426–121432.
[16] B.O. Rosseland, T.D. Eldhuset, M.J.E.G. Staurnes, Environmental effects of aluminium, Environ. Geochem. Health, 12 (1990) 17–27.
[17] A.E. Körlü, S. Yapar, S. Perinçek, H. Yılmaz, C. Bağıran, Dye removal from textile waste water through the adsorption by pumice used in stone washing, AUTEX Res. J., 15 (2015) 158–163.
[18] V.S. Munagapati, J.C. Wen, C.L. Pan, Y. Gutha, J.H. Wen, Enhanced adsorption performance of Reactive Red 120 azo dye from aqueous solution using quaternary amine modified orange peel powder, J. Mol. Liq., 285 (2019) 375–385.
[19] A.A. Adeyi, S.N. Jamil, L.C. Abdullah, T.S.Y. Choong, Adsorption of Malachite Green dye from liquid phase using hydrophilic thiourea-modified poly(acrylonitrile-co-acrylic acid): kinetic and isotherm studies, Hdw J. Chem., 7 (2019) 76–88.
[20] E. Erdem, N. Karapinar and R. Donat, The removal of heavy metal cations by natural zeolites, J. Colloid Interface Sci., 280 (2004) 309–314.
[21] N. Abidi, J. Duplay, A. Jada, E. Errais, M. Ghazi, K. Semhi, M. Trabelsi-Ayadi, Removal of anionic dye from textile industries' effluents by using Tunisian clays as adsorbents. Zeta potential and streaming-induced potential measurements, C.R. Chim., 22 (2019) 113–125.
[22] Z. Wang, M. Xue, K. Huang, Z. Liu, Textile Dyeing Wastewater Treatment, Advances in Treating Textile Effluent, InTechOpen, Shanghai, China, 5 (2011) 91–116.
[23] A. Gusso, N.A. Burnham, Investigation of the range of validity of the pairwise summation method applied to the calculation of the surface roughness correction to the van der Waals force, Surf. Sci., 651 (2016) 28–40.
[24] M. Naushad, Surfactant assisted nano-composite cation exchanger: development, characterization and applications for the removal of toxic Pb^{2+} from aqueous medium, Chem. Eng. J., 235 (2014) 100–108.
[25] A.A. Alqadami, M. Naushad, M.A. Abdalla, M.R. Khan, Z.A. Alothman, Adsorptive removal of toxic dye using Fe_3O_4–TSC nanocomposite: equilibrium, kinetic, and thermodynamic studies, J. Chem. Eng. Data, 61 (2016) 3806–3813.
[26] A.A. Alqadami, M. Naushad, Z.A. Alothman, T. Ahamad, Adsorptive performance of MOF nanocomposite for methylene blue and malachite green dyes: kinetics, isotherm and mechanism, J. Environ. Manage., 223 (2018) 29–36.
[27] A.A. Adeyi, S.N. Jamil, L.C. Abdullah, T.S.Y. Choong, K.L. Lau, M. Abdullah, Adsorptive removal of Methylene Blue from aquatic environments using thiourea-modified poly(acrylonitrile-co-acrylic Acid), Materials, 12 (2019) 1734–1751.
[28] V.S. Mane, P.V. Babu, Kinetic and equilibrium studies on the removal of Congo red from aqueous solution using *Eucalyptus* wood (*Eucalyptus globulus*) saw dust, J. Taiwan Inst. Chem. Eng., 44 (2013) 81–88.
[29] A.A. Adeyi, S.N. Jamil, L.C. Abdullah, T.S.Y. Choong, Hydrophilic thiourea modified poly(acrylonitrile co acrylic acid) adsorbent: preparation, characterization, and dye removal performance, Iranian Pol. J., 28 (2019) 483–491.
[30] I. Langmuir, The adsorption of gases on plane surfaces of glass, mica and platinum, J. Am. Chem. Soc., 40 (1918) 1361–1403.
[31] I. Mironyuk, T. Tatarchuk, M. Naushad, H. Vasylyeva, I. Mykytyn, Highly efficient adsorption of strontium ions by carbonated mesoporous TiO_2, J. Mol. Liq., 285 (2019) 742–753.
[32] S. Chegrouchea, A. Bensmailib, Removal of Ga(III) from aqueous solution by adsorption on activated bentonite using a factorial design, Water Res., 36 (2002) 2898–2904.
[33] S.B. Olugbenga, A.O. Mary, M.O, Abimbola, Sorption studies of lead ions onto activated carbon produced from oil-palm fruit fibre, Stem Cell, 42 (2010) 14–29.
[34] M.C. Manique, A.P. Silva, A.K. Alves, C.P. Bergmann, Titanate nanotubes produced from microwave-assisted hydrothermal synthesis: characterization, adsorption and photocatalytic activity, Braz. J. Chem. Eng., 34 (2017) 331–339.
[35] N. Atar, A. Olgun, F. Çolak, Thermodynamic, equilibrium and kinetic study of the biosorption of basic blue 41 using *Bacillus maceran*, Eng. Life Sci., 8 (2008) 499–506.
[36] K. Silas, W.A.W.A.-K. Ghania, T.S.Y. Choong, U. Rashid, Carbonaceous materials modified catalysts for simultaneous SO_2/NO_x removal from flue gas: a review, Catal. Rev., 61 (2018) 134–161.
[37] A.A. Alqadami, M. Naushad, Z.A. Alothman, A.A. Ghfar, Novel metal–organic framework (MOF) based composite material for the sequestration of U(VI) and Th(IV) metal ions from aqueous environment, ACS Appl. Mater. Interfaces, 9 (2017) 36026–36037.
[38] K. Silas, W.A.W.A.-K. Ghania, T.S.Y. Choong, U. Rashid, Optimization of activated carbon monolith Co_3O_4-based catalyst for simultaneous SO_2/NO_x removal from flue gas using response surface methodology, Combust. Sci. Technol., 58 (2019) 2–19.
[39] G. Lalitha, R. Hemamalini, M. Naushad, Efficient photocatalytic degradation of toxic dyes using nanostructured TiO_2/polyaniline nanocomposite, Desal. Wat. Treat., 108 (2018) 322–328.
[40] K. Silas, W.A.W.A.-K. Ghania, T.S.Y. Choong, U. Rashid, Breakthrough studies of Co_3O_4 supported activated carbon monolith for simultaneous SO_2/NO_x removal from flue gas, Fuel Process. Technol., 180 (2018) 155–165.
[41] A.U. Aydin, T.Y. Bysal, Remediation of Heavy metals in the Environ, CRC Press, Taylor and Francis, Florida, 2006.
[42] M. Naushad, Z.A. Alothman, M.R. Awual, S.M. Alfadul, T. Ahamad, Adsorption of rose Bengal dye from aqueous solution by amberlite Ira-938 resin: kinetics, isotherms, and thermodynamic studies, Desal. Wat. Treat., 57 (2016) 13527–13533.
[43] G. Sharma, M. Naushad, D. Pathania, A. Mittal, G.E. El-Desoky, Modification of *Hibiscus cannabinus* fiber by graft copolymerization: application for dye removal, Desal. Wat. Treat., 54 (2015) 3114–3121.
[44] Z.Z. Abidin, N. Ismail, R. Yunus, I.S. Ahamad, A. Idris, A preliminary study on *Jatropha curcas* as coagulant in wastewater treatment, Environ. Technol., 32 (2011) 971–977.
[45] B. Benguella, H. Benaissa, Effects of competing cations on cadmium biosorption by chitin, Colloids Surf., A, 76 (2002) 143–150.
[46] H.A. Chanzu, J.M. Onyari, P.M. Shiundu, Biosorption of malachite green from aqueous solutions onto polylactide/spent brewery grains films:kinetic and equilibrium studies, J. Polym. Environ., 45 (2012) 665–672.
[47] A.B. Albadarin, M.N. Collins, M. Naushad, S. Shirazian, G. Walker, C. Mangwandi, Activated lignin-chitosan extruded blends for efficient adsorption of methylene blue, Chem. Eng. J., 307 (2017) 264–272.
[48] E. Daneshvar, A. Vazirzadeh, A. Niazi, M. Kousha, M. Naushad, A. Bhatnagar, Desorption of Methylene blue dye from brown macroalga: effects of operating parameters, isotherm study and kinetic modeling, J. Cleaner Prod., 152 (2017) 443–453.
[49] T. Tatarchuk, N. Paliychuk, R.B. Bitra, A. Shyichuk, M. Naushad, I. Mironyuk, D. Ziółkowska, Adsorptive removal of toxic Methylene Blue and Acid Orange 7 dyes from aqueous medium using cobalt-zinc ferrite nanoadsorbents, Desal. Wat. Treat., 150 (2019) 374–385.
[50] C.H. Giles, T.H. MacEwan, S. Nakhwa, D.J. Smith, Studies in adsorption. Part XI. A system of classiscation of solution adsorption isotherms, and its use in diagnosis of adsorption mechanisms and in measurement of specific surface areas of solids, J. Chem. Soc. Ldn., (1960) 3973–3994, https://doi.org/10.1039/JR9600003973.
[51] C.H. Giles, A.P. D'Silva, I.A. Easton, A general treatment and classification of the solute adsorption isotherm part. II. experimental interpretation, J. Colloid Interface Sci., 47 (1974) 766–778.
[52] C. Namasivayam, R. Jeyakumar, R.T. Yamuna, Dye removal from wastewater by adsorption on 'waste' Fe(III)/Cr(III) hydroxide, Waste Mange., 14 (1994) 643–648.
[53] E. Lorenc-Grabowska, G. Gryglewicz, Adsorption characteristics of Congo Red on coal-based mesoporous activated carbon, Dyes Pigm., 74 (2007) 34–40.
[54] O. Sahu, N. Singh, Significance of Bioadsorption Process on Textile Industry Wastewater, In: The Impact and Prospects of Green Chemistry for Textile Tech., Woodhead Publishing, 34 (2019) 367–416.